END

FILMED

DTIC

MICROCOPY RESOLUTION TEST CHART

NATIONAL BUREAU OF STANDARDS-1963-A

REPORT DOCUMENTATION PAGE		READ INSTRUCTIONS BEFORE COMPLETING FORM
1. REPORT NUMBER NRL Memorandum Report 4975	2. GOVT ACCESSION NO. AD-A124 312	3. RECIPIENT'S CATALOG NUMBER
4. TITLE *(and Subtitle)* DESIGN OF ELECTRON-BEAM CONTROLLED SWITCHES		5. TYPE OF REPORT & PERIOD COVERED Interim report on a continuing NRL problem.
		6. PERFORMING ORG. REPORT NUMBER
7. AUTHOR(s) R. J. Commisso,* R. F. Fernsler,* V. E. Scherrer, and I. M. Vitkovitsky		8. CONTRACT OR GRANT NUMBER(s)
9. PERFORMING ORGANIZATION NAME AND ADDRESS Naval Research Laboratory Washington, DC 20375		10. PROGRAM ELEMENT, PROJECT, TASK AREA & WORK UNIT NUMBERS 61153N, RR0110941 47-0878-0-3
11. CONTROLLING OFFICE NAME AND ADDRESS Naval Research Laboratory Washington, DC 20375		12. REPORT DATE November 24, 1982
		13. NUMBER OF PAGES 29
14. MONITORING AGENCY NAME & ADDRESS *(if different from Controlling Office)*		15. SECURITY CLASS. *(of this report)* Unclassified
		15a. DECLASSIFICATION/DOWNGRADING SCHEDULE

16. DISTRIBUTION STATEMENT *(of this Report)*

Approved for public release, distribution unlimited.

17. DISTRIBUTION STATEMENT *(of the abstract entered in Block 20, if different from Report)*

18. SUPPLEMENTARY NOTES

*Present address: JAYCOR, Inc., 205 S. Whiting Street, Alexandria, VA 22302

19. KEY WORDS *(Continue on reverse side if necessary and identify by block number)*

Opening Switch
Repetitively Pulsed Operation
Electron Beam
Diffuse Discharges

20. ABSTRACT *(Continue on reverse side if necessary and identify by block number)*

This paper reviews the principles of operation of the electron-beam controlled switch (EBCS) and presents a procedure for its design. The EBCS is compared to other switches which have potential application to repetitively pulsed, high power systems, and is found to have some substantial advantages at high ($\geq$ 10 kHz) repetition rates. Circuit requirements for the application of an EBCS to ETA/ATA like devices are outlined. A self-consistent formalism for optimum switch design is derived. The formalism is applied to the previously outlined circuit requirements using capacitive and capacitive-inductive hybrid energy storage schemes. The required switches are readily designed.

DD FORM 1473 EDITION OF 1 NOV 65 IS OBSOLETE
1 JAN 73
S/N 0102-014-6601

CONTENTS

DESIGN OF ELECTRON-BEAM CONTROLLED SWITCHES

I. INTRODUCTION

Recent investigations[1-8] into the phenomena associated with electron-beam (e-beam) controlled diffuse discharges indicate potential applications for repetitive (>10 kHz in a "burst" mode), high power (~10^{10} W) switching. Applications include use in both the opening and closing switch mode. The switch requirements may vary considerably depending upon the specific mode used.

There now exists a need for the development of these switches in several areas. One area of focus is the generation and propagation of intense charged particle beams.[9] Here, the repetitive capability of the switch in the closing mode under high power operation is of critical importance. Another category of general interest is the development of a compact, high power inductive energy storage system to replace conventional capacitive systems.[10-12] This application has universal impact on many areas where pulsed power is required, including that of beam generation and propagation. In this case the generation of a high voltage pulse (>200 kV) as a result of the fast increase of an opening switch resistance while the switch is being stressed by high electric fields associated with the pulse is crucial. Depending upon the application, this opening switch may be repetitively pulsed. This would involve a more stringent set of requirements on both the switch gas and the switch e-beam driver than is the case for single pulse switching.

In this report we review the principles of operation of the e-beam controlled switch (EBCS), highlighting its capability for rapid recovery—the essential requirement for repetitively pulsed systems, whether inductively or capacitively driven. Detailed explanations of the switch physics can be found in Refs. 5, 8, 13, and 14. The EBCS is compared to other candidate switches for repetitive, high power application. Design requirements for two applications of this switch to devices with characteristics similar to either the Experimental Test Accelerator (ETA) or Advanced Test Accelerator (ATA)[15] are then outlined. We next develop a formalism for switch design that combines the circuit requirements with the switch physics. Using this formalism, which is backed by our present data base,[5,8,13,14] the necessary e-beam controlled switches are designed. The reader is cautioned that the design examples chosen do not necessarily make optimum use of the potential capabilities of the EBCS switch concept. A full system study in which the EBCS is included as an integral part of the design process from inception would be required for such a task. Rather, the examples chosen serve to illustrate the practical engineering aspects of the switches, define some of the technical requirements necessary for their implementation, and indicate the steps that are necessary for a complete system design.

The results of this study indicate that EBCS's can be readily designed for repetitive (>10 kHz), high power (200 kV, 20 kA) applications. Further research and development concerning gas chemistry and atomic physics, cumulative heating in the switch, and switch e-beam driver under repetitive, long conduction time (with respect to the load pulse width) conditions are needed in varying degrees depending upon the specific switch application. The authors believe that such studies will lead to further significant gain in the practicality of EBCS's.

II. PRINCIPLES OF OPERATION

When an electron beam is injected into a chamber containing a mixture of an attaching and a nonattaching gas, the ionization of the gas produced by the e-beam pulse competes with attachment and

recombination processes controlling the conductivity of the gas. The conductivity, and hence the discharge current, is turned on and off in association with the *e*-beam pulse.

An important distinguishing feature of a switch based on this concept is the ability of the switch to open (cease conduction) under high applied voltage. This is achieved by using the electron beam to control the gas ionization. To avoid avalanche ionization the switch must be designed so that the maximum expected voltage across the switch is below the static self-sparking threshold (for sufficiently transient voltages this requirement may be relaxed). As the discharge evolves, cumulative gas heating also must be constrained so that thermal ionization and, more importantly, local hydrodynamic reduction in gas density do not significantly lower the self-sparking threshold. A self-sustained discharge is thus prevented. Under these conditions, the fractional gas ionization, and thus the switch resistivity, at any time is determined by the competition between ionization provided by the beam and the various recombination and attaching processes characteristic of the specific gas mixture, pressure, and applied electric field. A second important feature of this switch is the volume discharge property. This characteristic makes it possible to avoid excessive heating of electrodes and the switch gas (as well as lessen mechanical shock and minimize the switch inductance). All these features combine to permit the discharge to return to its initial state of high resistivity very quickly once the source of ionization is removed. Unlike an arc discharge, this transition can be accomplished rapidly in the presence of an applied voltage. Some details of the gas chemistry and atomic physics associated with the switch operation and their coupling to the switch circuitry can be found in Ref. 8.

Looked at from a different perspective, the EBCS behaves as a current amplifier. That is, the small (≤ 1 kA) electron beam current can control a large (~ 10 kA) switch plasma current. The ratio of these two currents is called the current gain, ϵ. For $\epsilon \gg 1$ a substantial energy gain (i.e., energy delivered to the load normalized to the energy dissipated) can be achieved, as discussed in Sec. V.

III. COMPARISON TO OTHER SWITCHES

Several summaries of high power closing and opening switches with potential application to repetitively pulsed systems exist.[9,16] There are basically six switch types which emerge as candidates for a high power repetitively pulsed switch:[9] (1) the low-pressure gas switch,[17] (2) the surface flashover switch,[18] (3) the thyratron,[9,16] (4) the high pressure spark gap, (5) the magnetic switch,[19,20] and (6) the EBCS.

The ongoing research for both the low pressure gas and surface flashover closing switches has yielded some encouraging results. The technology appears to be simple. At present, however, recovery times of only 100 μs have been observed for both devices with no applied voltage. Jitter may also be a problem. Under repetitive burst operation, both switches may have to be cooled. For the surface flashover switch, the insulator may additionally require cooling and the insulator lifetime is likely to be limited.

The thyratron is a well developed device; however, the present limitations in voltage, current, and risetime probably make it unsuitable for implementation in the systems of interest here. Further, the power consumption and long warm up period for the cathode heater are disadvantageous.

The high pressure spark gap is the traditional choice for a closing switch of the pulsed power community. It cannot be used as an opening switch. It is very simple mechanically and has associated with it an extensive data base. The problem areas are the substantial gas flow requirements and energy dissipation associated with this device when used in high frequency repetitive high power applications. Also, a trigger pulse amplitude comparable to the applied switch voltage is necessary for low jitter.

Magnetic switches are now a part of the ATA design. The potential advantages of such a switch are its simplicity, ruggedness, and lifetime. Questions still remain concerning overall size and weight,

2

evaluation of core materials, limiting output pulse duration, pulse compression ratios, trade-offs in number of stages in cascade, and core bias and/or resetting methods.

An understanding of the physics of the e-beam switch operation along with the results of recent NRL experiments leads one to conclude that the principal advantages of the EBCS are: (1) rapid recovery (opening) of the switch when the electron beam ceases, and the consequent opening and closing repetitive capability[8,13,14] at high repetition rates; (2) negligible switch jitter;[4,5] (3) volume discharge resulting in low inductance and reduced switch current density (limiting electrode wear, switch gas heating, and mechanical shock); and (4) high power switching capability[5] (for limited pulse bursts).

Potential problem areas for this switch concept include the switch e-beam driver complexity, the effect of cumulative heating on the switch's repetitive capability, and switch packaging. The e-beam driver has modest peak power requirements on a per-pulse basis (200 kV, <1 kA, <10^8 W); however, it must provide a beam with the pulse shape and repetition rate required for the desired switching characteristics. Thermionic e-beam generators, developed for excitation of high power lasers, now provide[21,22] 1-5 μs e-beam pulses with ~100 ns rise and decay times at a 25 Hz repetition and at 10 A/cm^2. The repetition rate can probably be improved, e.g., if a lower e-beam current density is desired. With some further development, these devices may indeed provide the desired beam modulation characteristics. Thin film field emission cathodes with molybdenum cones[23] appear attractive because of their low control voltage (100-300 V), high current densities (~10 A/cm^2), and continuous operation capability. An inductively driven electron beam system has successfully demonstrated two-pulse "burst" operation, generating two ~1 kA pulses with a 150-200 μs (limited by diode closure) interpulse separation.[24] In regard to the EBCS and the role of the e-beam source we quote from Ref. 9 (pg. 439), "The main application of this switch concept would seem to be as an opening switch. Since it has few rivals in this role, the complexity of the electron beam source becomes less formidable."

The effects of cumulative heating in the switch gas are not well known. Preliminary experiments[14] indicate that at least two-pulse operation is possible at a deposited energy density of ~0.1 J/cm^3. These experiments also show a favorable (approximately linear) scaling of the maximum energy deposited before switch breakdown occurs with increasing switch ambient pressure. However, more research in this area is needed.

Although a stand-alone switch packaging scheme has been outlined,[25] a complete system design has not yet been addressed. Such a design would be heavily dependent on the specific application and would have to incorporate the switch as an integral part of the system ab initio. At present we see no fundamental limitation resulting from packaging considerations that would prevent integration of this switch into pulse power systems. For example, a compact, high pressure, e-beam controlled laser system with an e-beam generator (single pulse) compatible with severe optical requirements has been successfully assembled and operated.[26]

Much work is still needed to develop these concepts into viable repetitively operated switches. In some areas (e.g., recovery) the EBCS has some very substantial advantages when compared to the other switch candidates. It is the only switch discussed here that can open under an applied voltage and, therefore, it is especially promising in applications which require high repetition rate (>10 kHz) opening switches.

IV. DESIGN CRITERIA

In this section we outline switch performance characteristics upon which a switch can be designed. These characteristics strongly depend upon the specific application of the switch. Optimum switch performance requires that the switch be incorporated into a system design at its inception. However, to illustrate the practical design considerations for this switch concept we have chosen as an example the

requirements of the ETA/ATA inductive electron beam accelerator.[15] In this context we describe the requirements for application of this switch to three energy storage schemes: capacitive, hybrid, and inductive. Depending upon the specific requirements, each scheme may involve, respectively, a more stringent set of switch performance and e-beam driver characteristics and a progressively greater extrapolation from the present data and technology base.

A. Capacitive Systems—Application of the Repetitive Closing Switch Mode

The e-beam controlled switch based on the principles outlined in Sec. II can be used at high power levels ($\sim 10^{10}$ W) with capacitive energy storage as a closing switch, in applications where very fast rise-time pulses of short duration (<100 ns) must be generated at high repetition frequency (>10 kHz).

1. Switch Electrical Characteristics for Closing Switch

One example of such an application is an output switch of the ETA/ATA. For definition purposes, the load characteristics are assumed to be those summarized in Table I.[15]

The characteristics displayed in Table I imply that the switch e-beam driver has sufficiently fast risetime and that the working gas can respond sufficiently fast to the injected beam.

Two circuits which provide the required output for the load are shown in Fig. 1a and b. Both circuits depend on use of switch S_1 for charging. Typically, direct Marx charging as given in Fig. 1a can provide a charge time for capacitor C_o, of $\tau_{CH} \sim 1$ μsec. Using the voltage step-up transformer (Fig. 1b) has no deleterious effect other than to possibly increase τ_{CH} to several microseconds.

Electrically, the switch must deliver a peak power $P = 4 \times 10^9$ W to the load for each pulse. With >10 kHz repetition rate (<100 μsec pulse-to-pulse separation), the average power output of the pulse is $P_{av} = P(\tau_L/\tau_{pp}) = 1 \times 10^6$ W, where τ_L is the load pulse width and τ_{pp} is the time between pulses. (For those scenarios where large numbers of accelerating modules are needed, the total average output power can be as high as 1×10^9 W.) The power transport through the switch leads to some dissipation of energy in the switch. The amount that is dissipated depends on the pulse duration, the current, and the switch voltage drop during conduction and is constrained to be less than the energy delivered to the load (see Sec. V.A.2). The opened state of the switch has negligible conduction in all cases considered in this paper.

Finally, the switch inductance must be limited to $L_{SW} << V_L \tau_R/I_L \simeq 100$ nH, as suggested by the parameters in Table I. A schematic representation of the time history of the switch resistance, R_{sw}, is shown in Fig. 1c.

TABLE I: SUMMARY OF ASSUMED
LOAD CHARACTERISTICS
(Closing Switch, Capacitive System)

Type of Load	Electron beam diode
Load Voltage, V_L	200 kV
Load Current, I_L	20 kA
Equivalent Impedance, R_L	10 Ω
Pulse Duration, τ_L	40 ns
Pulse Rise Time, τ_R	10 ns
Pulse-to-Pulse Time, τ_{pp}	<100 μs
Pulses per burst, n	$\geqslant 5$

4

CAPACITIVE (CLOSING)
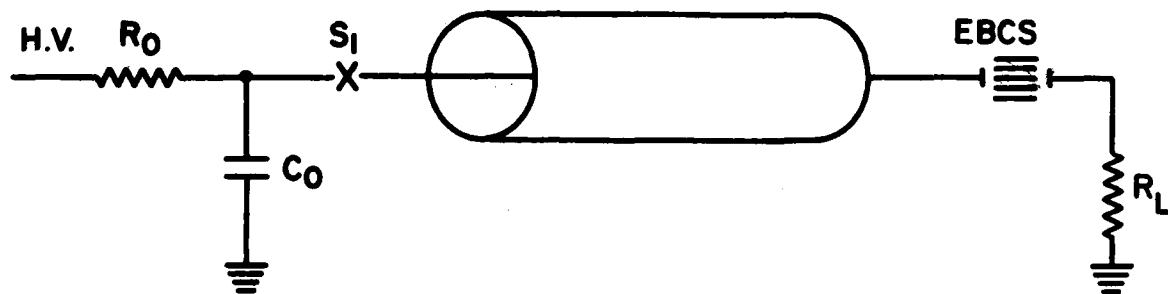
(a)
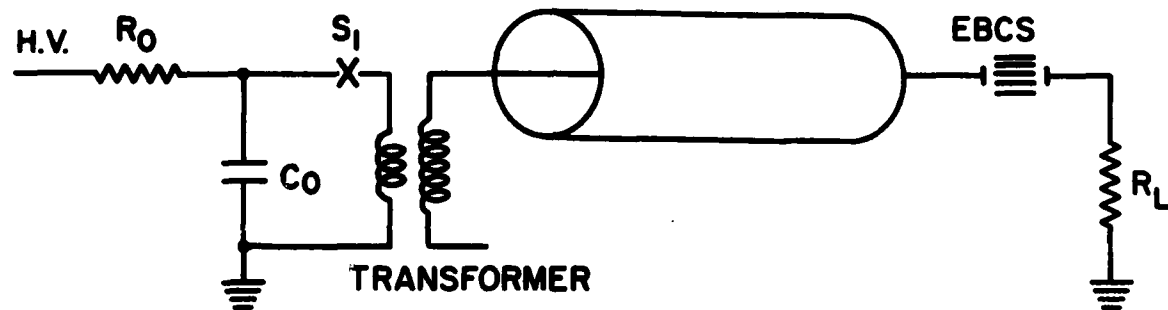
(b)

(c)

Fig. 1 — Circuit diagram illustrating the application of an EBCS in the closing mode to a capacitive storage system. The circuit is shown both without (a) and with (b) a step-up transformer. Also shown is a representation of the switch resistance time behavior (c).

2. Electron Beam Requirements

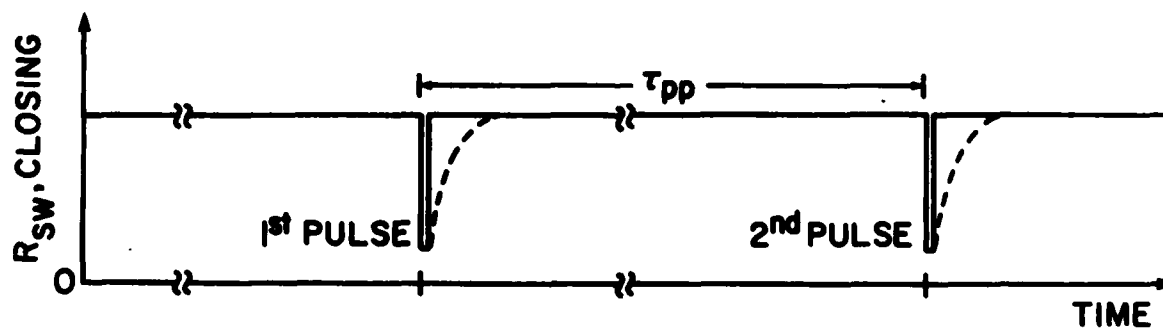To obtain the necessary time variation of the gas conductivity, the electron beam injected into the gas must satisfy pulse shape, repetition rate, and current requirements. The e-beam current is set by a number of factors, as discussed in Sec. V. The beam modulation was discussed in Sec. III. We assume for the remainder of the discussion that an appropriate e-beam generator exists, or can be developed.

B. Inductive Systems—Application of Repetitive Opening Switch Mode

In projecting charged particle beam technology to deployable systems, practical size and weight of the system is one of the major considerations in the system design. The power source represents a major component of any of the proposed systems. Because inductive storage offers a potential for much more compact designs than those that would be possible with capacitive systems, there exists a strong incentive to develop the necessary inductive storage components. A repetitive opening switch is a fundamental component that must yet be developed. As in the repetitive closing switch development, e-beam control of gas conductivity offers a method that can be employed for repetitive opening switching for high power pulse train production.

1. Hybrid Pulser

Continuing with the scenario of an accelerator based on modular accelerating sections requiring 20 kA, 200 kV, and 40 nsec pulses at a burst rate of >10 kHz, the power supply circuits, shown in Figs. 2 and 3, can be employed.

The circuit in Fig. 2a utilizes a pulse-forming line, represented as a capacitor C, to form a specific pulse shape required by the accelerator (i.e., rise time of 10 nsec and 40 nsec pulse duration). The inductor, L_o, is initially charged by a current, I_o, through, in this example, an explosively actuated switch[27-28] (denoted by E) for a time τ_{CH}^o. Note that some current generators, e.g., a homopolar, may require earlier, additional stages of pulse compression. When switch E opens, the current is commutated (in a time τ_{COM}) to the next stage which contains an EBCS operating in the repetitive opening mode (denoted by the letter O in parenthesis). EBCS(O) is closed and conducting during τ_{COM}. After the commutation time, EBCS(O) is commanded to open. The opening generates a resistive voltage, and the pulse line C is charged for the charging time, $\tau_{CH} = \tau_L$. At the end of τ_{CH}, EBCS(O) again closes.

The output for the pulse line is an e-beam controlled device already described in the previous section, i.e., an EBCS operating in the repetitive closing mode (denoted by letter C in parenthesis). Figure 2b is a schematic representation of the time histories of the resistance of EBCS(O) and EBCS(C) of Fig. 2a.

Thus, the circuit in Fig. 2a employs two repetitive EBCS's. The EBCS(O) has a long conduction time, equal to $\tau_C = (\tau_{pp} - \tau_{CH})$, and a short nonconduction time, $\tau_{NC} = \tau_{CH}$, during which the capacitor C is charged. The EBCS(C) is identical in its operation to the switch discussed in Sec. IV.A.

2. Inductive Pulser

A more compact and simpler pulser would result if a circuit in Fig. 3a could be used. The pulser represented by this circuit is purely inductive, eliminating any need for capacitive storage. However, this scheme represents the farthest extrapolation of the present data and technology base thus far considered. Figure 3b is a schematic representation of the time history of the opening switch resistance for a purely inductive system of Fig. 3a. The EBCS(O) in Fig. 3a must conduct for the period between pulses, τ_{pp}, and open repetitively for a much shorter period, τ_L. The output pulse shape, however, imposes stringent performance requirements on EBCS(O), in terms of pulse risetime and duration.

HYBRID (OPENING/CLOSING)

(a)

(b)
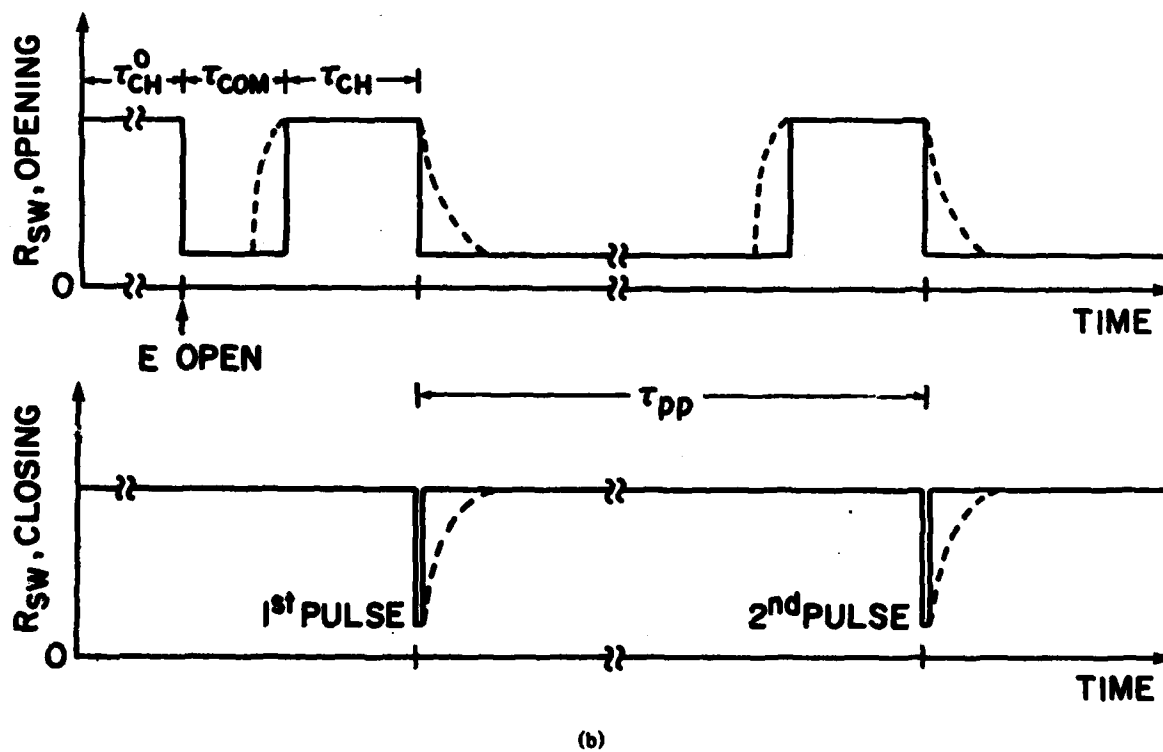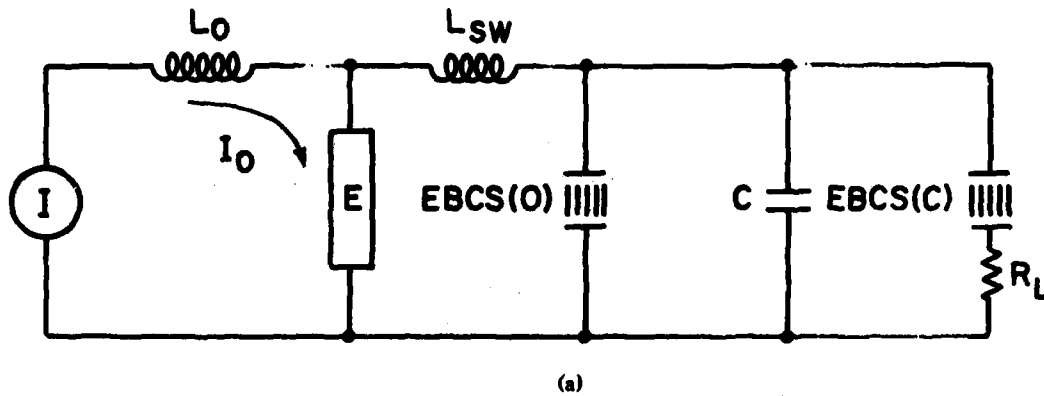
Fig. 2 — Circuit diagram illustrating the application of an EBCS in the opening mode, EBCS(O), and closing mode, EBCS(C), for a hybrid (capacitive-inductive) inductive storage system (a). Also shown are representations of the time behavior of both switch resistances (b).

7

INDUCTIVE (OPENING)

(a)

(a)

(b)

(b)
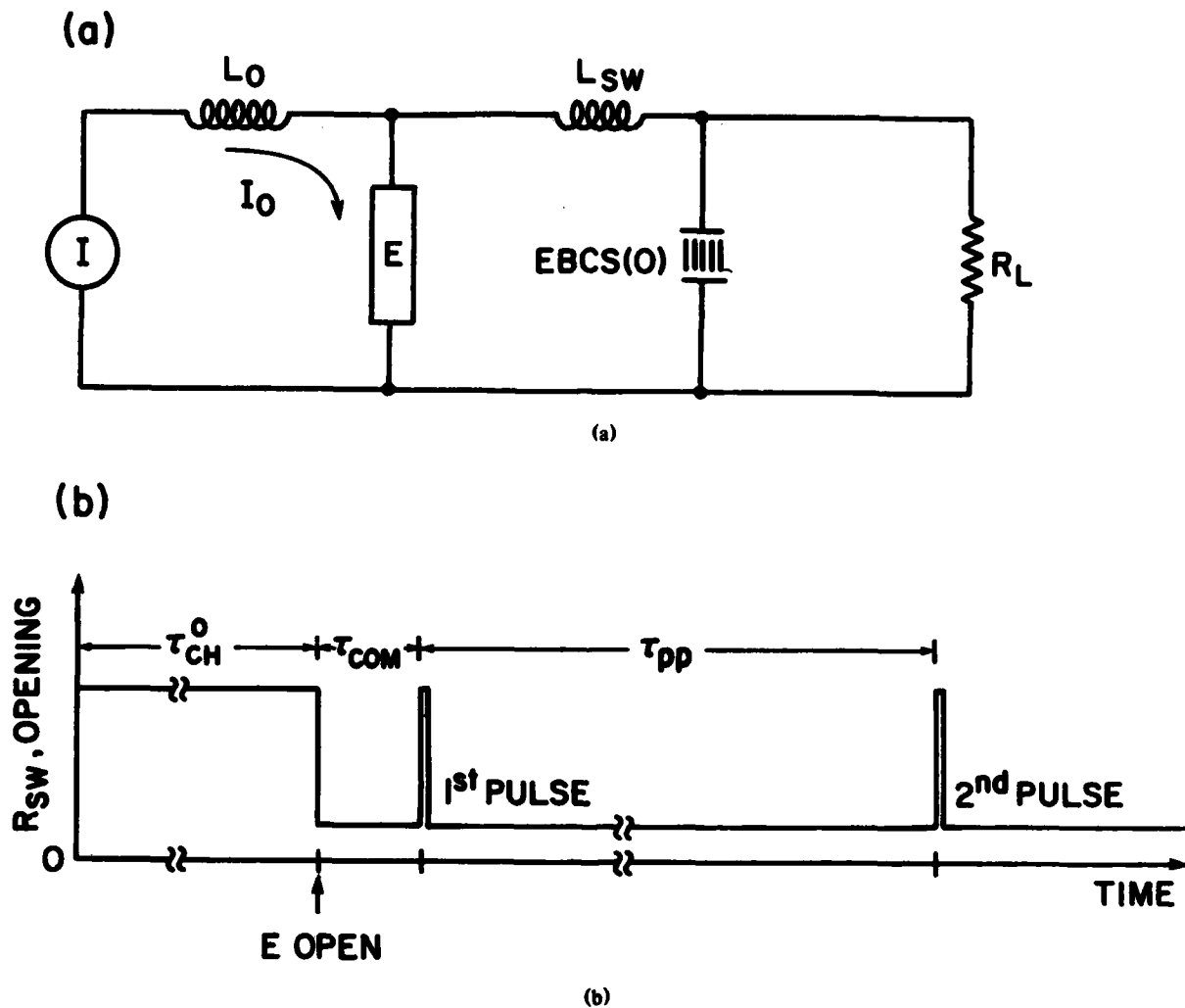
Fig. 3 — Circuit diagram illustrating the application of an EBCS in the opening mode for a purely inductive energy storage system (a). Also shown is a representation of the switch resistance time behavior (b).

8

Although this scenario is conceptually the simplest, it may be too speculative to assume that a single switch can achieve an opening time of less than 10 ns and a conduction time of greater than 10 μs. Thus, this design is not considered for detailed engineering at present. The option of using a purely inductive system is attractive and, therefore, suggests that future effort should be invested in development of switches with opening times of ~10 nsec. We note that response times of <10 ns are theoretically possible[5]; however, an e-beam driver with the necessary waveform capability needs to be developed.

3. Electrical Characteristics for Opening Switch—Hybrid System

The energy associated with a single pulse for a single module delivering 20 kA, at 200 kV, with a 40 nsec pulse width, is very small: $E_1 = 160$ J. Considering a 10-pulse burst, ~2 kJ is required as a minimum to be stored by the inductor. Taking 30% efficiency of conversion from stored to pulse energy, ~6 kJ must be handled by a storage system for charging one pulse line. This projects to ~10^7 J for a 1000 module accelerator. In considering the engineering of a switching system, one must know the number of modules to be powered by one switch. At this stage of switch development, where little experience with a practical switching device exists, the choice is dictated as much by the need to maintain a reasonable experimental set-up as by the lack of certainty related to the ultimate application. A reasonable first attempt, that would uncover most of the problems of a design, would be a switch design for a 10-module pulse train generator limited to 5-pulses. Circuit, current, and voltage parameters are derived below for the EBCS(O) switch of Fig. 2a.

Using the same final load pulse parameters as in the preceding section, the single pulse line capacity is $C = 2E_1/V^2 = 8$ nF; i.e., in 10-module operation 80 nF must be charged to 200 kV. Choosing a 5-burst pulse train for an initial switch design (and for experiment design to test the switch), the total stored energy in the ten pulse lines is $E_2 = 8$ kJ. We assume a 15 μs interpulse time (~70 kHz) and a 2-μs charge time. The energy stored in the inductor must be about $E_3 = 3 \times E_2 = 24$ kJ, to account for the inefficiencies (~70%) associated with the circuit and fuses shown in Fig. 2a. This amount of energy suggests that low voltage capacitors can be conveniently used as the source of current (shown in Fig. 2a) to charge the inductor in small laboratory experiments. As previously stated, the time required to pulse-charge the capacity C, is taken to be $\tau_{CH} = 2$ μsec. This is consistent with compact water-dielectric pulse line requirements. The current needed to charge a capacitance to a given voltage, V, is $I_o = dQ/dt = CV/\tau_{CH}$. For $C = 80$ nF, $V = 200$ kV and $\tau_{CH} = 2$ μs, $I_o = 8$ kA. The storage inductor $L_o = 2 E_3/I_o^2 = 750$ μH. This choice of inductor presents no structural or electrical design problems.

To summarize, the EBCS(O) of Fig. 2a charging the ten pulse-lines must accommodate the circuit performance characteristics shown in Table II.

TABLE II: Summary of Assumed
Circuit Characteristics
(Opening Switch, Hybrid System)

Type of Load	Capacitive
Peak voltage, V_L	200 kV
Load current, $I_L = I_o$	8 kA
Conduction time, $\tau_C = (\tau_{pp} - \tau_{CH})$	13 μs
Nonconduction time, $\tau_{NC} = \tau_{CH}$	2 μs
Storage Inductance, L_o	750 μH
Pulses per burst, n	5

9

V. SWITCH DESIGNS

In this section we apply the results of experimental and theoretical research at NRL and the switch performance criteria described previously to obtain specific switch designs. First we review the important switch characteristics and their relationship to the system. A simple quantitative model for the switch physics along with scaling relations is then presented. A design procedure is outlined that self-consistently incorporates the switch electrical characteristics with switch physics. Finally, the values of the switch parameters are obtained and the closing and opening switches are designed.

A. Switch Parameters

The following switch parameter considerations are of importance for opening and closing switch designs.

1. Breakdown

If the electric field across the switch exceeds the static breakdown field at the ambient switch pressure, the switch may go into an arc mode, which is undesirable because it prevents the switch from opening. This leads to the constraint that

$$V_L = s_B \frac{E_B^o}{P_o} (Pl), \qquad (1)$$

where V_L is the maximum expected voltage across the switch (i.e., the load voltage), E_B^O is the static breakdown field at atmospheric pressure P_o, $s_B < 1$ is a dimensionless safety factor, and l is the switch length. We have assumed that $E_B = E_B^o (P/P_o)$, where E_B is the static breakdown field at pressure P. This condition can be relaxed somewhat for transient, <1 μs, pulses.

Additionally, cumulative heating of the gas must be sufficiently constrained so that any local reduction in switch gas density does not significantly lower the self-sparking threshold. Energy is deposited in the switch from the following processes:

(1) During the time the switch changes from a conducting to a nonconducting state, i.e., during the opening time τ_O, the current in the switch is finite while the switch resistance is large. Thus, the resistive heating during this time may be significant. This cumulative heating is estimated by

$$H_O = k_O I_{SW} V_L n \tau_O, \qquad (2)$$

where I_{SW} is the maximum switch current, V_L is the maximum switch voltage (load voltage), n is the number of pulses, τ_O is the opening time, and $k_O \leqslant 0.5$ is a dimensionless constant which appropriately averages $(I_{SW} V_L)$ during τ_O (see Sec.V.C). Because $\tau_O \gg \tau_{SR}$, where the switch rise time, τ_{SR}, is the time for the switch to change from nonconducting to conducting, we will neglect the energy loss during the switch closing phase.

(2) During the total time the switch is conducting, $n\tau_C$, there will be some resistive heating. The total energy deposited in the switch as a result of this process is approximated by

$$H_C = I_{SW}^2 R_{SW} n \tau_C. \qquad (3)$$

Here R_{SW} is the switch resistance during conduction.

(3) When the beam is injected, a fraction of the beam energy will be directly deposited in the switch gas as a result of inelastic collision processes. This energy deposition is estimated by

$$H_b = k_b I_b V_b n \tau_C. \qquad (4)$$

10

where I_b and V_b are the beam current and voltage respectively, and $k_b \leqslant 1$ is the fraction of the beam energy deposited in the switch (determined from V_b, P, and l). The conduction time τ_C is also the e-beam pulse duration.

To properly constrain cumulative heating in the switch, we must have

$$H_O + H_C + H_b < W_B A l. \tag{5}$$

Here W_B is the deposited energy per unit volume at which the self-sparking threshold is altered and A is the switch area. As shown in Fig. 4, W_B scales linearly with ambient gas pressure P.[14] We therefore take $W_B = (P/P_o) W_B^0$, where $W_B^0 \simeq 0.15$ J/cm^3 is the breakdown energy density at atmospheric pressure.[5,14,29] Equations (2)-(5) can thus be combined to give

$$\left[k_O I_{SW} V_L \left[\frac{\tau_O}{\tau_C} \right] + I_{SW}^2 R_{SW} + k_b I_b V_b \right] n \tau_C = s_H \left[\frac{W_B^0}{P_o} \right] A (Pl), \tag{6}$$

where $s_H \leqslant 1$ is a dimensionless safety factor.

2. Efficiency

The switch energy gain, ξ, is defined as the ratio of the energy delivered to the load to the total energy used in making the switch conduct. Thus, applying the same arguments used in obtaining Eqs. (2)-(4) we have

$$\xi = \frac{I_L V_L \tau_L}{\left[k_O I_{SW} V_L \left[\frac{\tau_O}{\tau_C} \right] + I_{SW}^2 R_{SW} + I_b V_b \right] \tau_C}, \tag{7}$$

where I_L is the load current and τ_L is the load pulse width e.g., $\tau_L = \tau_{CH}$ for the opening switch of the hybrid system in Figs. 2a and 3b, while for closing switch $\tau_L = \tau_C$, see Figs. 1 and 3a. In all cases, $I_{SW} = I_L$ (although not always at the same time).

The switch efficiency, η, is related to ξ by $\eta = \xi/(\xi + 1)$. Thus, to attain a high efficiency,

$$\xi > 1. \tag{8}$$

Upon substitution of $I_L = I_{SW}$ and using the definition of current gain, $\epsilon \equiv I_{SW}/I_b$, Eq. (7) becomes

$$\xi = \frac{(\tau_L/\tau_C) \epsilon}{[(\tau_O/\tau_C) k_O + (I_{SW} R_{SW}/V_L)] \epsilon + 1}. \tag{9}$$

Recently obtained measurements of ϵ as a function of percent O_2 in N_2 for 1, 2, and 3 atm at an applied $E/P = 10.5$ V/cm-torr with an e-beam current density of 5 A/cm^2 are illustrated in Fig. 5. Because of the short duration (200 ns) and long rise time (100 ns) of the e-beam pulse used in these measurements, the values of $\epsilon \lesssim 15$ at low O_2 concentrations (<20%) should be considered a lower bound.[14]

Equation (7) may be rearranged to yield

$$\xi^{-1} I_L V_L \tau_L = k_O I_{SW} V_L \tau_O + I_{SW} V_L \tau_C + I_b V_b \tau_C. \tag{11}$$

To realize an energy gain, i.e., for $\xi > 1$, each term on the right hand side of Eq. (11) must be sufficiently less than $I_L V_L \tau_L$. Thus we set

$$k_O I_{SW} V_L \tau_O = g_O I_L V_L \tau_L, \tag{12a}$$

$$I_{SW}^2 R_{SW} \tau_C = g_C I_L V_L \tau_L. \tag{12b}$$

and

$$I_b V_b \tau_C = g_b I_L V_L \tau_L, \tag{12c}$$

where g_O, g_C, $g_b < 1$, such that

$$\xi^{-1} = g_O + g_C + g_b < 1. \tag{13}$$

Equations (12a)-(12c) can be rewritten (with $I_{SW} = I_L$) as:

$$\tau_O = (g_O/k_O)\tau_L, \tag{14a}$$

$$\frac{E_C}{P} = g_C s_B (E_B^o/P_o) \frac{\tau_L}{\tau_C}, \tag{14b}$$

and

$$\epsilon = g_b^{-1} \frac{V_b}{V_L} \left[\frac{\tau_C}{\tau_L} \right], \tag{14c}$$

where $E_C = I_{SW} R_{SW}/l$ is the electric field across the switch during conduction.

3. Resistance

The switch resistance during conduction is related to the switch gas resistivity during conduction, ρ_o, by

$$R_{SW} = \rho_o \frac{l}{A}. \tag{15}$$

Plotted in Fig. 6 is the resistivity at peak switch current as a function of percent O_2 in N_2 for 1, 2 and 3 atm at an applied $E/P = 10.5$ V/cm-torr for an e-beam current density of 5 A/cm^2. Values of 300-400 Ω-cm are typical for <20% O_2. We reiterate that because of the short duration (200 ns) and relatively long rise time (100 ns) of the electron beam used in the experiment, the values of ρ_o in Fig. 6 for low concentrations of O_2 can be considered as an upper bound (see Ref. 14).

By recalling that $E_C = I_{SW} R_{SW}/l$ and using Eq. (1) to eliminate l, we may rewrite Eq. (14b) as

$$R_{SW} = g_C \left[\frac{V_L}{I_{SW}} \right] \frac{\tau_L}{\tau_C} \tag{16}$$

for the switch resistance during conduction. This equation and the condition $g_C < 1$ is essentially equivalent to the requirement that the characteristic L/R time of the system be long compared to the switch conduction time, so that the current will not resistively decay from the system.

4. Closing and Opening Times

The characteristic time scale for the switch to change from nonconducting to conducting is the switch closing time, τ_{SR}. This time is important in closing switch designs (Fig. 1) and for our experiments has been limited by the beam rise time ($\sim$100 ns) and the circuit parameters. When fast rising (<5 ns) beams were used, rise times as short as 2 ns have been observed.[4]

The characteristic time scale for the switch to change from a conducting to a nonconducting state is the opening time, τ_O. On this time scale the switch current decreases and switch resistance increases by orders of magnitude.

12
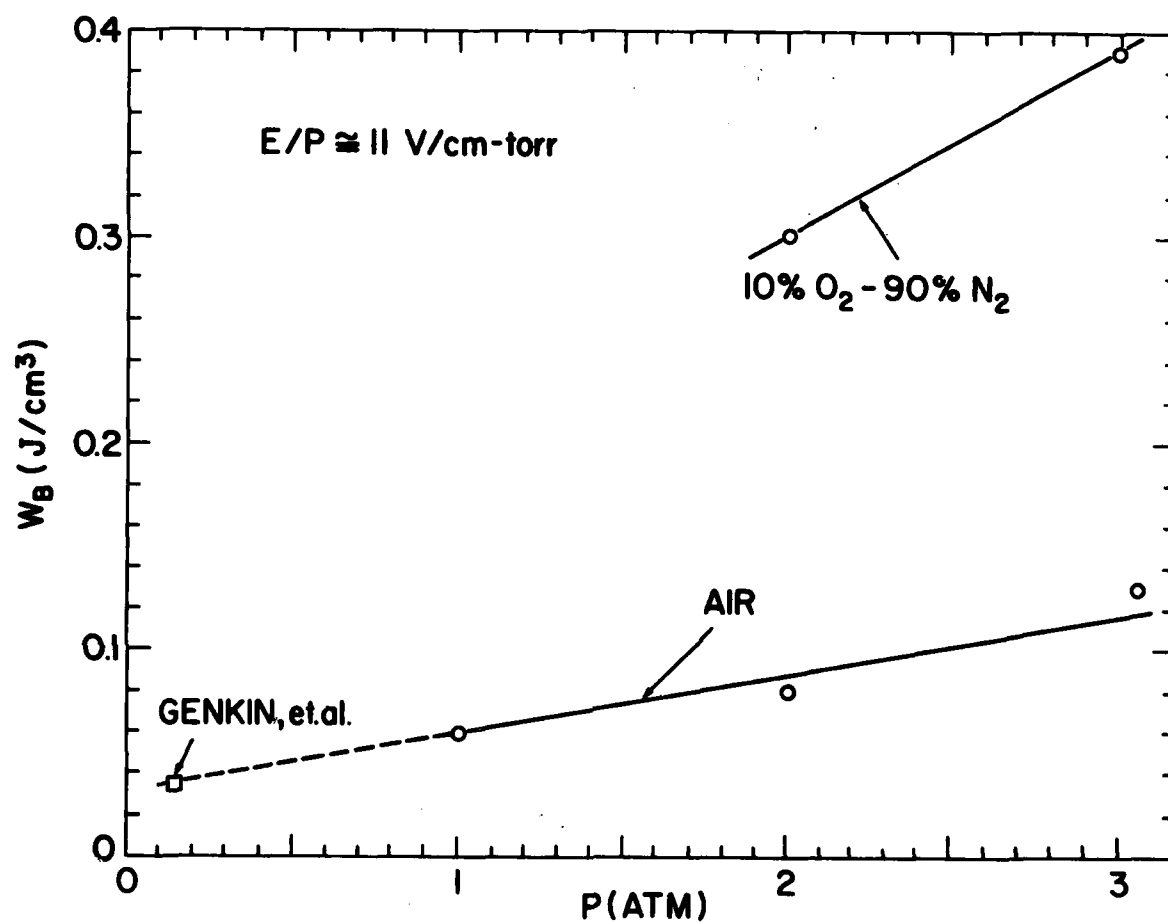
Fig. 4 — Plot of deposited energy density required for breakdown, W_B, as a function of ambient pressure, P, for Air and a 10% O_2-90% N_2 mixture. Genkin, et al. is given in Ref. 29.

Fig. 5 — Plot of current gain, ϵ, as a function of O_2 concentration in N_2 at $E/P = 10.5$ V/cm-torr and $J_b = 5$ A/cm^2 for ambient pressure $P = 1$, 2 and 3 atm.

14

Fig. 6 — Plot of resistivity at peak switch current, ρ_o, as a function of O_2 concentration in N_2 at $E/P = 10.5$ V/cm-torr and $J_b = 5$ A/cm^2 for ambient pressure $P = 1$, 2 and 3 atm.

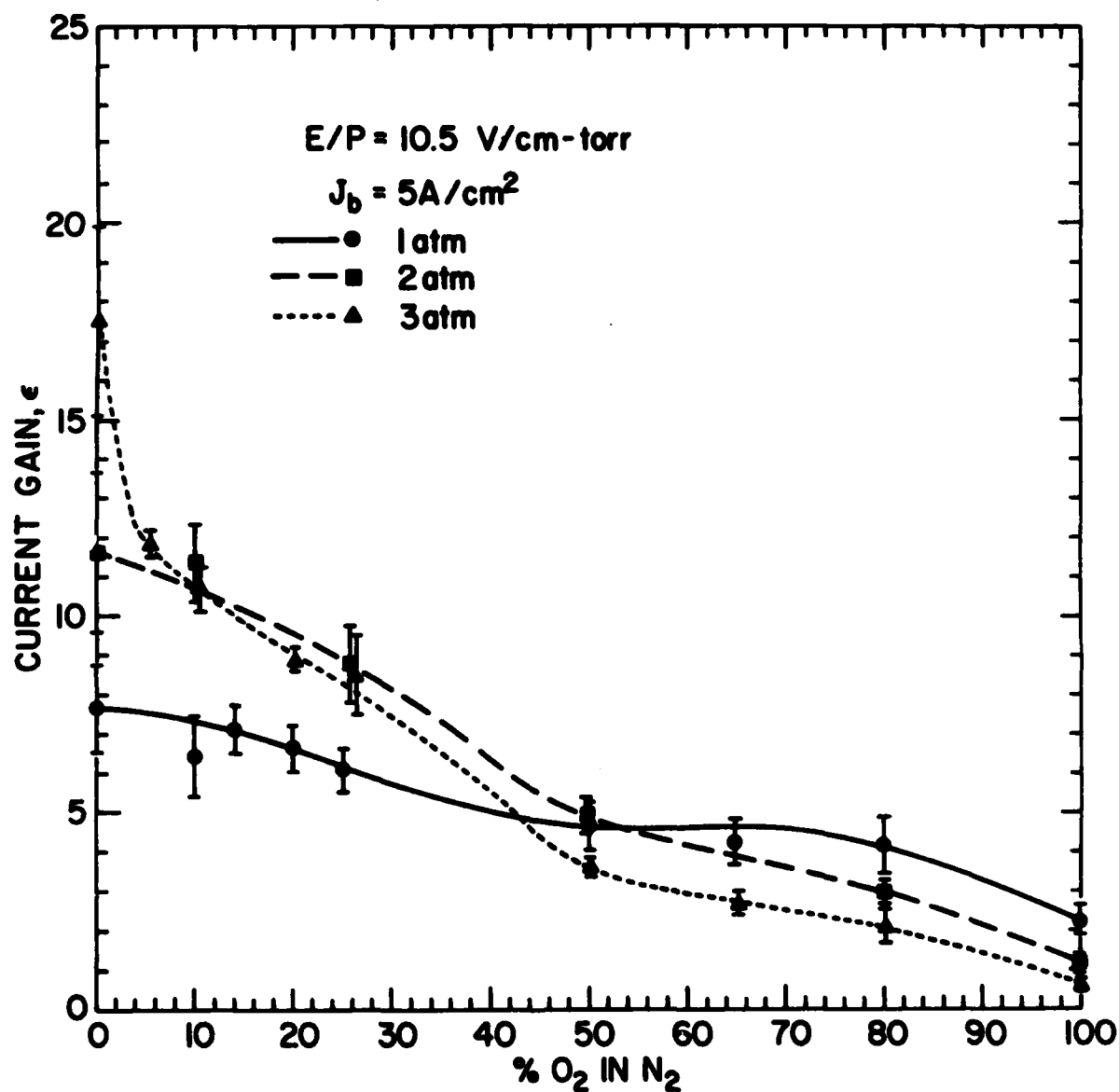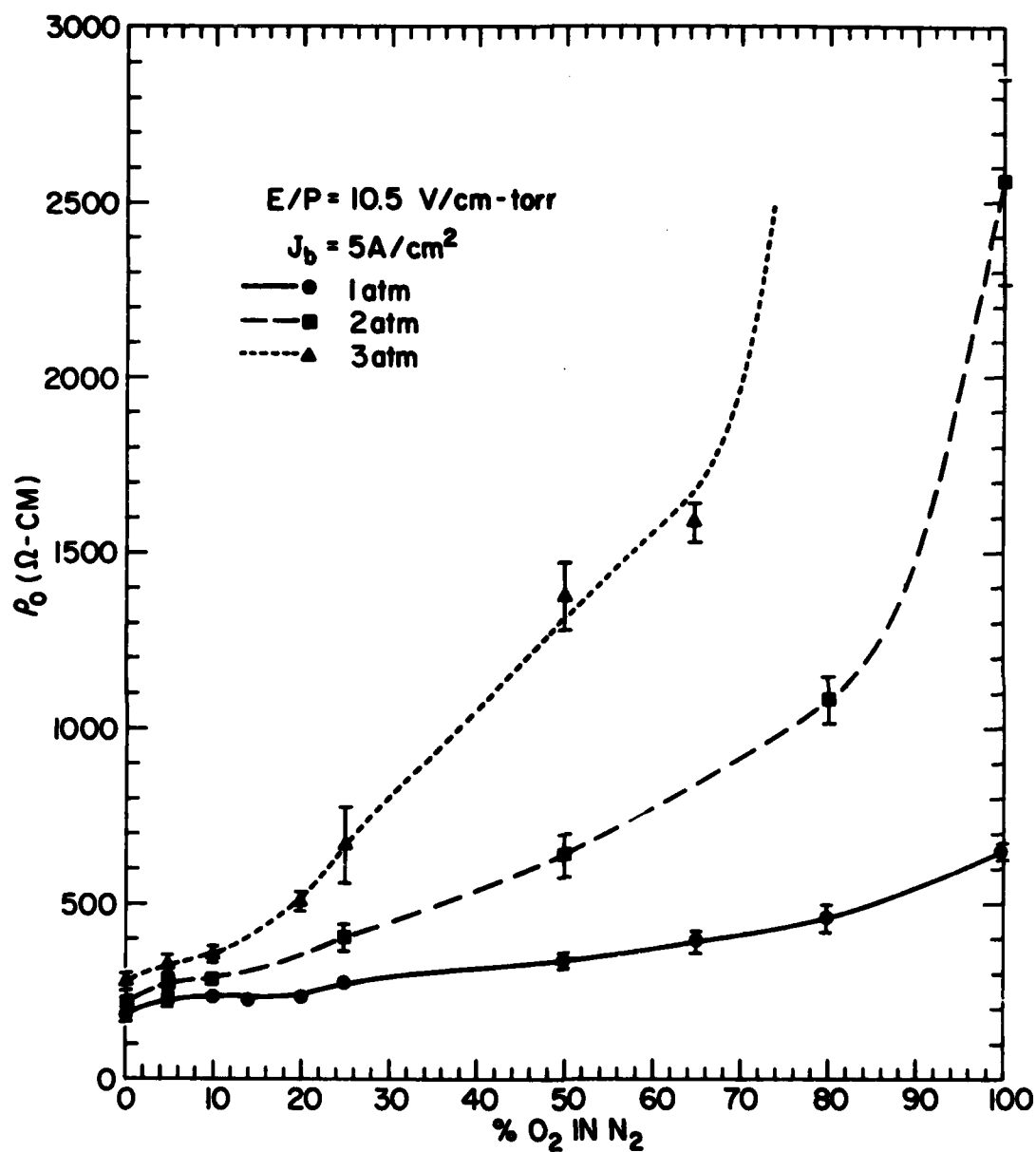Values of τ_O obtained from single pulse experiments[8,13,14] are plotted in Fig. 7 as a function of O_2 concentration in N_2 at 1, 2 and 3 atm with an applied $E/P = 10.5$ V/cm-torr for an e-beam current density of 5 A/cm². For this plot, τ_O was estimated from the inductively generated voltage, V_l, by $\tau_O \approx L\Delta I/V_l$, where ΔI is the change in the system current and L is the system inductance. Typically, values of $\tau_O \leqslant 300$ ns, limited by the beam decay time (~ 100 ns) are observed.

B. Switch Physics

The continuity equation for the switch plasma electron density, n_p, can be expressed simply as[14]

$$\frac{dn_p}{dt} = S_o P J_b - \frac{n_p}{\tau_p}, \tag{17}$$

where $J_b \equiv I_b/A$ is the e-beam current density and τ_p is the characteristic loss time for the switch plasma electron density. Several to very many τ_p periods are necessary for the switch to open, depending upon the dominant mechanism responsible for switch plasma electron loss. Thus, we have

$$\tau_O = k_p \tau_p, \tag{18}$$

where $k_p \approx 5$ for an attachment dominated switch or $k_p \approx 10^2 - 10^3$ for a recombination dominated switch.[5]

S_o is a beam ionization parameter given by

$$S_o = \frac{1}{e\epsilon_i P_o}\left[\frac{dE}{dX}\right]_o, \tag{19}$$

where e is the electronic charge, $\epsilon_i \simeq 35$ eV is the energy required for ionization per electron-ion pair, and $(dE/dX)_o \simeq 3$ keV/cm is the energy lost per unit length for the beam electrons at 1 atm.

The plasma density is related to the switch plasma current density through

$$J_{SW} \equiv I_{SW}/A = n_p e v, \tag{20}$$

where v is the electron drift velocity,

$$v = \mu E. \tag{21}$$

Here μ is the electron mobility[30] and E is the electric field across the switch. Thus the resistivity during conduction is given by

$$\rho_o = \frac{E_C}{J_{SW}} = (e n_p \mu)^{-1}. \tag{22}$$

Substituting n_p from Eq. (22) into Eq. (17), and noting that at equilibrium $dn_p/dt = 0$, Eq. (17) becomes

$$J_b \rho_o \tau_p = f_o^{-1}, \tag{23}$$

where $f_o \equiv e S_o \mu P$ is essentially a constant for a given gas composition. For most gases $f_o \sim 10^5 - 10^6$ cm/V-s. Note that Eq. (23) indicates that for a given beam current and gas with a constant f_o, there is a "trade-off" between resistivity and opening time.

Finally, using the definition of ϵ, J_{SW}, and J_b, Eq. (23) can be expressed as

$$\frac{\epsilon}{\tau_p} = E_C f_o. \tag{24}$$

The relations derived in this section are used to relate the switch physics to the switch circuit characteristics outlined in Sec. V.A.
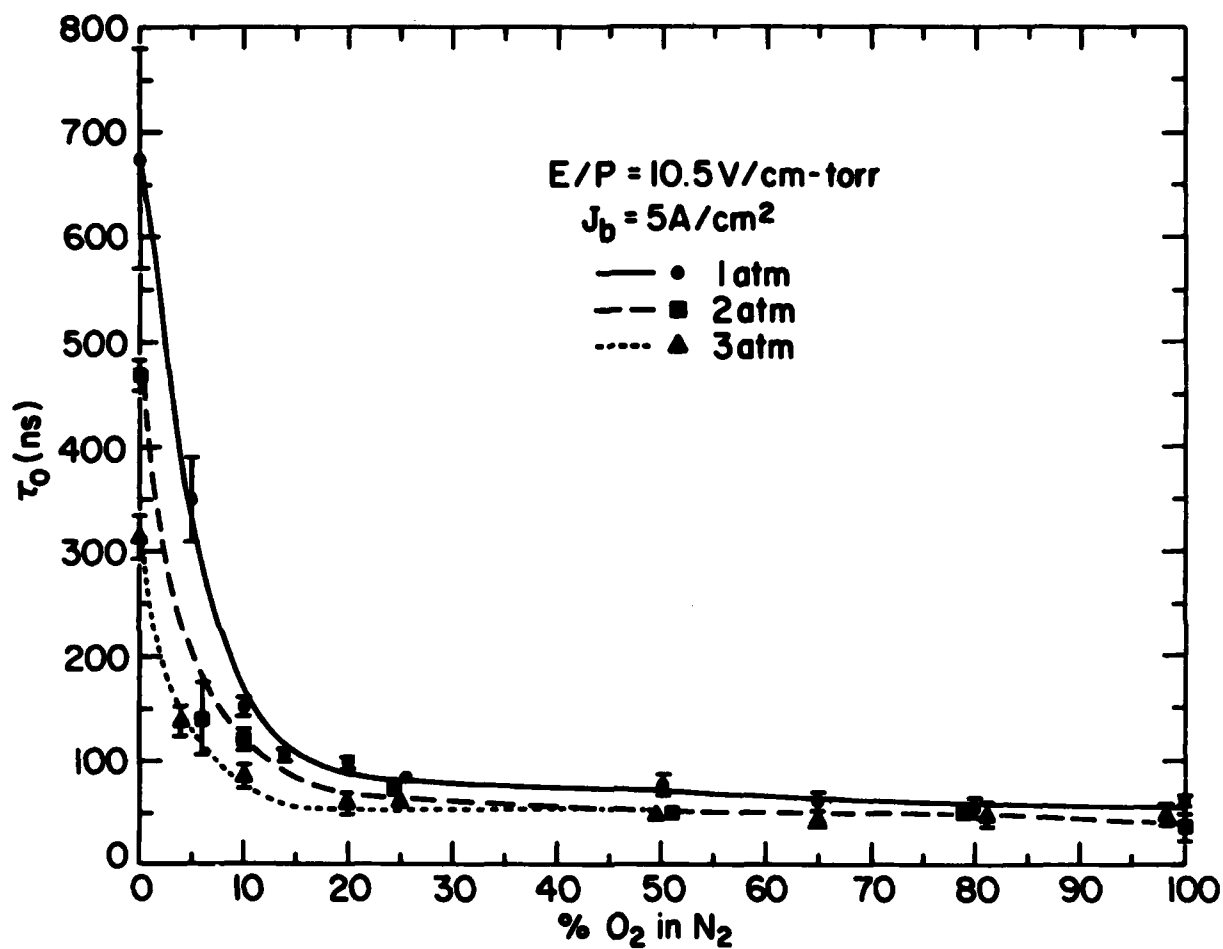
16

Fig. 7 — Plot of switch opening time, τ_o, as a function of O_2 concentration in N_2 at $E/P = 10.5$ V/cm-torr and $J_b = 5$ A/cm^2 for ambient pressure $P = 1$, 2 and 3 atm.

C. Design Procedure

In this section we combine the switch circuit requirements with the switch physics to develop a self-consistent procedure for obtaining the switch gas composition and pressure, the switch length, and switch area (radius) for a given switch gain.

First we obtain the factor k_O in Eq. (2), which when multiplied by the power delivered to the load gives the average power dissipated by the switch during the opening phase. During the time the switch is undergoing a transition from conducting to a nonconducting state (τ_O), the switch current is decreasing and the switch resistance is increasing. During τ_L the switch current changes by I_{SW} $(= I_L)$ and switch voltage changes by V_L; thus we define

$$k_O \equiv \frac{<I_{SW}> <V_{SW}>}{I_{SW} \; V_L},\tag{25}$$

where $<I_{SW}>$ and $<V_{SW}>$ are the average values of the switch current and voltage during τ_O.

The time history of the voltage across the switch will depend upon the load voltage time behavior (see Figs. 1 and 2). For loads where the load voltage rises to its peak value in a time $\simeq \tau_O$ (i.e., resistive or inductive loads), $<I_{SW}> \simeq 1/2 \; I_{SW}$ and $<V_{SW}> \simeq 1/2 \; V_L$ so that

$$k_O \simeq 1/4.\tag{26}$$

For a capacitive load (Fig. 2a), the load voltage reaches its maximum in a time $\tau_L = \tau_{CH}$. In this case, we still have $<I_{SW}> \simeq 1/2 \; I_{SW}$. However, $<V_{SW}> \simeq <I_{SW}> \tau_O/2C = V_L \tau_O/4\tau_L$. Thus, for a capacitive load,

$$k_O \simeq 1/8 \; (\tau_O/\tau_L).\tag{27}$$

Once k_O is known, the opening time, τ_O can be computed from Eq. (14a) for a choice of g_O. Knowing τ_O, Eq. (18) can be used along with data on attachment and recombination rates, to make a judgement on whether the switch should be attachment or recombination dominated, thus suggesting a specific gas composition. The value obtained for τ_O must be also consistent with the circuit requirements. If not, the choice of g_O must be modified.

We now set out to compute the switch pressure. Beginning with Eq. (14b) and substituting for E_C from Eq. (24), for ϵ from Eq. (14c), for τ_p from Eq. (18), and for τ_O from Eq. (14a) we obtain

$$P^{-1} = \frac{g_O g_C g_b s_B f_o}{k_O k_p} \; \tau_L \; \frac{E_B^2}{P_o} \left[\frac{V_L}{V_b}\right] \left[\frac{\tau_L}{\tau_C}\right]^2.\tag{28}$$

The factors g_O, g_C, and g_b are chosen so that P can be made small consistent with the constraint of Eq. (13). An optimum choice for g_O, g_C, and g_b can be obtained by using the method of Lagrange undetermined multipliers,[31] with the result that $g_O \simeq g_C \simeq g_b = g$ (note that in some cases k_O and k_p can depend on the g factors). For example, if a ξ of 3 is chosen then $g \simeq 0.1$ and $\eta = 0.75$.

Once P is known, Eq. (1) gives the switch length

$$l = \frac{V_L}{s_B P (E_B^2/P_o)}.\tag{29}$$

The value chosen for V_b in Eq. (28) can be combined with P and l to compute k_b of Eq. (4). Note that in order for the beam to traverse the switch length V_b will depend on the product Pl, as does V_L. Therefore, one can show that typically $V_b \simeq V_L$, with $k_b \simeq 0.3$.

18

The electron beam current to be injected into the switch can be obtained from Eq. (14c) and the definition of current gain, ϵ:

$$\epsilon \equiv I_{SW}/I_b = g_b^{-1} \frac{V_b}{V_L} \left[\frac{\tau_C}{\tau_L} \right]. \tag{30}$$

By substituting R_{SW} from Eq. (16) and I_b from Eq. (30) into Eq. (6) we arrive at the required switch area:

$$A = \frac{I_{SW} V_L (n\tau_L) g_C}{s_H (W_B^g/P_o) Pl} \left[1 + \frac{k_O}{g_C} \left[\frac{\tau_O}{\tau_L} \right] + k_b \frac{g_b}{g_C} \right]. \tag{31}$$

The area thus computed insures that the switch will be large enough that the total energy per unit volume deposited in the switch is less than the deposited energy density required to lower the break-down threshold.

The e-beam generator requirements are determined from V_b, I_b, and A. I_b is computed from Eq. (30). The e-beam generator must actually provide a somewhat higher current than I_b to account for current lost to the structure supporting the vacuum-high pressure interface. The e-beam generator must also supply a beam of area A.

D. Design for Repetitive Closing Switch—Capacitive System

Taking the circuit parameters described in Table 1, we apply the results of Sec. V.C to arrive at a switch design for the repetitive closing switch of Fig. 1.

For this case we choose $\tau_{pp} = 15\ \mu s$, safety factors $s_B = 0.75$, $s_H = 0.5$, and $V_b = 200$ kV. As previously stated (Table II) $I_{SW} = I_L = 20$ kA, $n = 5$, $V_L = 200$ kV, and $\tau_L = 40$ ns. Choosing $\xi = 2$ gives $g_O \simeq g_C \simeq g_b = 0.17$. With $\tau_C = \tau_L = 40$ ns, Eq. (30) requires $\epsilon \simeq 6$. Because the load is not capacitive we substitute k_O from Eq. (26) into Eq. (14a) to compute τ_O:

$$\tau_O \simeq 4g_O\tau_L \simeq 30 \text{ ns}. \tag{32}$$

It is not disturbing that $\tau_O \sim \tau_L$ because the pulse line does most of the load pulse shaping; therefore, the major requirements are that $\tau_O < \tau_{pp}$ and that $\tau_{SR} \leq \tau_R$. The second requirement can be easily met for an e-beam risetime $\leq \tau_p$.[4] We choose k_p in Eq. (18) to be ~ 5 (attachment dominated) so that the plasma electron decay time $\tau_p \approx 6$ ns. This can be achieved with a N_2-O_2 gas mixture of 4:1.[5]

The switch pressure is given by Eq. (28) with $E_B^g \simeq 20$ kV/cm, $f_o = 2 \times 10^5$ cm/V-s for N_2-O_2 and $k_O = 0.25$ (Eq. (26)):

$$P \simeq 1700 \text{ Torr} \simeq 2.3 \text{ atm}. \tag{33}$$

The switch length is then (Eq. (29))

$$l \simeq 5.9 \text{ cm}. \tag{34}$$

These l, P, and V_b values are consistent with $k_b \simeq 0.3$.

Equation (31) is then used to obtain the switch area (radius)

$$\begin{aligned} A &\simeq 2590 \text{ cm}^2 \\ (r &\simeq 29 \text{ cm}), \end{aligned} \tag{35}$$

giving a switch current density of $J_{SW} \simeq 8$ A/cm². The e-beam current density is thus $J_b \simeq 1.3$ A/cm². From Eq. (16) we compute $R_{SW} \simeq 1.7\ \Omega$ and from Eq. (15) we obtain $\rho_o = 745\ \Omega$-cm.

19

Table III is a summary of the values of the switch parameters which, along with the required switch inductance ($\leqslant 100$ nH), completely characterize the switch.

The e-beam generator is required to deliver ≥ 20 J/pulse with a very fast rise and decay time. The e-beam current density, however, is modest, ~ 1 A/cm^2.

E. Design for Repetitive Opening Switch—Hybrid System

Taking the circuit parameters described in Table II, we apply the results of Sec. V.C to arrive at a switch design for the repetitive opening switch EBCS(O) of Fig. 2.

For this case: $\tau_{pp} = 15$ μs, $\tau_{NC} = \tau_L = 2$ μs, $I_{SW} = I_L = I_o = 8$ kA, $n = 5$, and $V_L = 200$ kV (Table II). We choose $s_B = 0.75$, $s_H = 0.5$, and $V_b \simeq V_L = 200$ kV. Setting $\xi = 4$ gives 'Eq. (13)) $g_O \simeq g_C \simeq g_b = 0.08$. With $\tau_C \simeq \tau_{pp} - \tau_L$, Eq. (30) requires $\epsilon \simeq 80$. Because of the capacitive load, we substitute k_O from Eq. (27) into Eq. (14a) to compute τ_O:

$$\tau_O = \sqrt{8 g_O}\, \tau_L \simeq 1.6 \ \mu\text{s}. \tag{36}$$

Since $\tau_O \sim \tau_L$, a substantial fraction of the final charge voltage for the capacitor will be attained during the opening time. This presents no serious problems, because the major requirement is that the capacitor be charged in a time $\leq \tau_{pp}$. We choose k_p in Eq. (18) to be ~ 5 (attachment dominated) so that $\tau_p \approx 300$ ns, which can be readily attained using N_2 with a small ($\sim 1\%$) admixture of O_2.

The switch pressure is given by Eq. (29) with $f_o = 2 \times 10^5$ cm/V-s for N_2 and $k_O = 0.1$ (Eq. (27)):

$$P = 5230 \text{ Torr} \simeq 7 \text{ atm}. \tag{37}$$

The switch length is then (Eq. (29))

$$l = 1.9 \text{ cm}. \tag{38}$$

Equation (31) is then used to obtain the switch area (radius):

$$A = 3000 \text{ cm}^2$$
$$(r \simeq 31 \text{ cm}), \tag{39}$$

giving a switch current density of $J_{SW} \simeq 2.6$ A/cm^2. The e-beam current density is thus $J_b \simeq 0.03$ A/cm^2. At this point the switch resistance can be computed as in Sec. V.D.

Table IV summarizes the values of the switch parameters, which, along with a required switch inductance (~ 5 μH), completely characterize the switch.

The e-beam generator requirements are quite modest with only 2.6 J/pulse needed. This reduces the complexity of the e-beam pulse modulation. The pressure requirement may be relaxed by as much as an order of magnitude by choosing a gas with a higher mobility during conduction, e.g., a mixture of Ar with O_2 or CH_4 with an attaching gas (CO_2). Alternately, use of these gases will increase the switch efficiency if the switch pressure can remain high, as is evident from Eq. (28). This is an area where more research is needed.

VI. CONCLUDING REMARKS

We had three principal objectives in the present paper. The first was to review the principles of operation of electron-beam controlled switches, emphasizing the ability of these switches to recover and open rapidly under high applied voltage. This rather unique capability makes the EBCS attractive, particularly when compared with other switch candidates, as either a single pulse opening switch or as a switch for repetitively pulsed systems with high repetition rates.

20

Table III — Characteristics of Closing Switch
for a Capacitive Pulser

A. Switch Parameters

gas	$N_2:O_2 \sim$ 4:1
pressure, P	2.3 atm
length, l	5.9 cm
Area (radius), $A(r)$	2590 cm^2 (29 cm)
Current Density, J_{SW}	8 A/cm^2
energy gain (current gain), $\xi(\epsilon)$	2(6)
resistance during conduction	1.7 Ω
voltage drop during conduction	34 kV

B. E-Beam Parameters

voltage, V_b	200 kV
current, I	3.5 kA
risetime $\leq \tau_p$	$\leq$2 ns
decay time $\leq \tau_O$	$\leq$30 ns

Table IV — Characteristics of Opening Switch
for a Hybrid Pulser

A. Switch Parameters

Gas	$N_2:O_2 \sim$ 99:1
Pressure, P	7 atm
length, l	1.9 cm
Area (radius), $A(r)$	3000 cm^2 (31 cm)
current density, J_{SW}	2.6 A/cm^2
Gain (current gain), $\xi(\epsilon)$	4(80)
Resistance during conduction, R_{SW}	0.3 Ω
Voltage drop during conduction	2.4 kV

B. E-Beam Parameters

Voltage, V_b	200 kV
current, I_b	100 A
rise and decay time, $\leq \tau_p$	$\leq$100 ns

The second objective was to present a formalism for switch design. The formalism given emphasizes the overall energy-transfer efficiency of the switch, the fundamental circuit requirements, and the switch physics. Our analysis indicates that efficiencies of $\simeq 80\%$ should be achievable for the examples chosen. We point out that these efficiencies are conservative in that the switch designs utilize the well known but nonoptimum gases, N_2 and O_2. Significant improvements in switch energy gain should result if N_2 were replaced by a gas such as CH_4 with high electron mobility, or if O_2 were replaced by a gas such as C_2F_6 in which the attachment rate increases rapidly with applied field.

The third objective was to illustrate the capabilities of the EBCS in a parameter regime of interest, both as an opening switch for inductive energy store, and as a fast closing switch. In the examples chosen, the opening switch would conduct for $\sim 15~\mu s$ and open in $\sim 1~\mu s$; the closing switch would close in ~ 5 ns and conduct for ~ 50 ns. The switch size in both cases was roughly one-half meter in diameter by a few cm in length.

Although single pulse operation has not been stressed in this report, it is important to note that the EBCS is capable of providing opening times substantially shorter than what can be achieved with wire fuses, the only available alternative for fast opening applications. New developments in erosion switches[32] may provide a fast opening time, but the conduction times are limited. Therefore, from the standpoint of the general development of inductive storage, the EBCS may make a significant contribution.

We stress that the performance of any EBCS is primarily limited by the desired switch efficiency and by the ambient switch gas pressure, as indicated by Eqs. (13) and (28). Choosing nominal values for k_O, k_p, s_B, E_B^0/P_o, recalling the switch efficiency $\eta = \xi/(\xi + 1)$, and assuming $V_b \simeq V_L$, Eq. (28) can be rewritten as

$$\left(\frac{\tau_C}{\tau_L}\right)^2 \approx 0.6\,P\left(\frac{1 - \eta}{\eta}\right)^3 f_o \tau_L. \tag{40}$$

The reader is reminded that f_o is proportional to the electron mobility. Equation (40) indicates that as η is made large, τ_C/τ_L becomes smaller. This type of relationship will exist for any opening switch, because there are always losses associated with the conduction phase.

As an example, we choose an energy efficiency of 80% ($\eta = 0.8$), $f_o = 2 \times 10^6$ cm/V-s, and assume a maximum practical gas pressure of 10 atm. Equation (40) then becomes

$$\left(\frac{\tau_C}{\tau_L}\right)^2 \lesssim \tau_L/(1~\text{ns}). \tag{41}$$

This condition precludes sub-nanosecond load pulse widths. That is, for a closing switch ($\tau_L \simeq \tau_C$), $\tau_L \gtrsim 1$ ns. In the case of an opening switch this condition additionally limits the maximum allowed conduction time, τ_C. For instance, for a load (open) time of $\tau_L = 1~\mu s$, the switch conduction time is limited to $\tau_C \leqslant 30~\mu s$. By reducing the switch efficiency to 50%, however, a conduction time of $\tau_c \leqslant 250~\mu s$ could be realized. Equation (41), along with the similar equation for 50% efficiency, is displayed graphically in Fig. 8.

This report has not addressed all issues of concern to EBCS design and operation. We have not discussed, for example, the impact of electrode sheath effects, current conduction by ions, or vacuum interface problems. Nonetheless, none of these additional issues should seriously compromise the design performance. This statement is supported by experiments performed at NRL and elsewhere.[1-4,6-8,13,14] These experiments, which cover a wide parameter space, demonstrate that the EBCS does indeed open under high applied voltage and that the simple models used are adequate to explain the observed switch behavior.
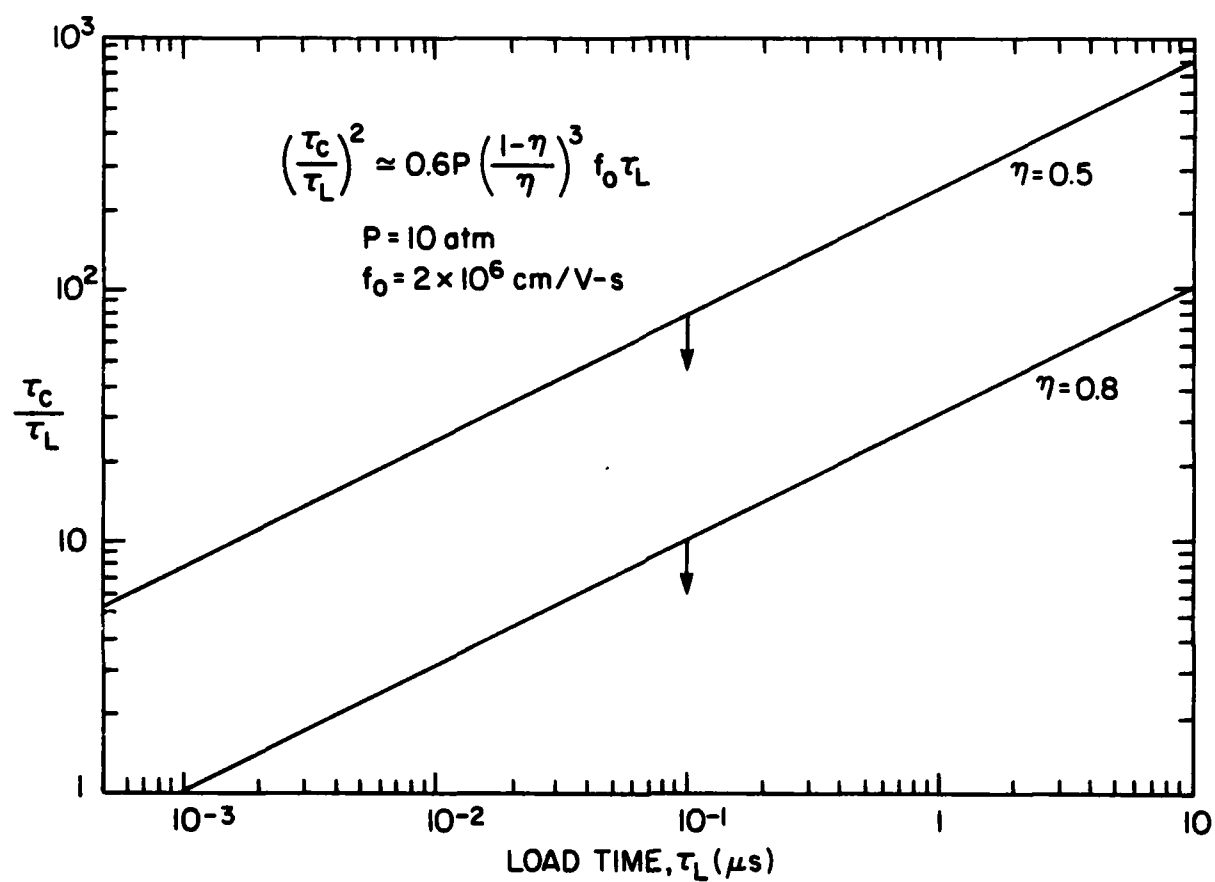
Fig. 8 — Plot of τ_C/τ_L as a function of τ_L based on Eq. (28) for switch efficiences. η of 0.5 and 0.8

VII. REFERENCES

1. R.O. Hunter, Proc. International Pulsed Power Conference, Lubbock, TX (1976), IC8:1-6.

2. J.P. O'Louglin, Proc. International Pulsed Power Conference, Lubbock, TX (1976), IIIC5:1-6.

3. B.M. Kovalchuk and G.A. Mesyats, Sov. Tech. Phys. Lett., 2, 252 (1976).

4. K. McDonald, M. Newton, E.E. Kunhardt, M. Kristiansen, and A.H. Guenther, IEEE Trans. Plasma Sci. PS-8, 181 (1980).

5. R.F. Fernsler, D. Conte and I.M. Vitkovitsky, IEEE Trans. Plasma Sci. PS-8, 176 (1980).

6. P. Bletzinger, Proc. of Workshop on Repetitive Opening Switches, Tamarron, Colorado, Texas Tech University Rept. (April 1981), p. 128.

7. Lawrence E. Kline, Proc. of Workshop on Repetitive Opening Switches, Tarrarron, Colorado, Texas Tech University Rept. (April 1981), p. 121.

8. R.J. Commisso, R.F. Fernsler, V.E. Scherrer, and I.M. Vitkovitsky, IEEE Trans. Plasma Sci., to be published (1982).

9. J. Benford, Physics International Co., San Leandro, CA, private communication (1980).

10. J. Salge, V. Braunsberger, and V. Schwartz, 1st International Conference on Energy Compression and Switching, Torino (1974).

11. I.M. Vitkovitsky, D. Conte, R.D. Ford, and W.H. Lupton, NRL Memorandum Report 4168 (1980).

12. R.D. Ford, D. Jenkins, W.H. Lupton, and I.M. Vitkovitsky, Rev. Sci. Inst. 52, 694 (1981).

13. V.E. Scherrer, R.J. Commisso, R.F. Fernsler, L. Miles, and I.M. Vitkovitsky, Third International Symposium on Gaseous Dielectrics, Knoxville, TN (1982).

14. V.E. Scherrer, R.J. Commisso, R.F. Fernsler, and I.M. Vitkovitsky, 1982 Fifteenth Power Modulator Symposium, Baltimore, MD (1982).

15. W.A. Barletta, Lawrence Livermore Laboratory Report, UCRL-87288 (1981).

16. T.R. Burkes, J.P. Craig, M.O. Hagler, M. Kristiansen, and W.M. Portnoy, IEEE Trans. Elect. Dev. ED-26, 1401 (1979).

17. E.J. Lauer and D.L. Birx, Third IEEE International Pulsed Power Conference, Albuquerque, NM IEEE Cat. No. 81CH1662-6 (1981), pg. 380.

18. I.D. Smith, G. Lauer, and M. Levine, 1982 Fifteenth Pulse Power Modulator Symposium, Baltimore, MD (1982).

19. D.L. Birx, et al., 1982 Fifteenth Pulse Power Modulator Symposium, Baltimore, MD (1982).

20. D.L. Birx, E.J. Laurer, L.L. Reginato, D. Rogers, Jr., M.W. Smith, and T. Zimmerman, Third IEEE International Pulsed Power Conference, Albuquerque, NM, IEEE Cat. No. 81CH1662-6 (1981), p. 262.

21. J.E. Eninger, Third IEEE International Pulsed Power Conference, Albuquerque, NM, IEEE Cat. No. 81CH1662-6 (1981), p. 499.

22. A.W. Freidman and J.E. Eninger, Third IEEE International Pulsed Power Conference, Albuquerque, NM, IEEE Cat. No. 8ICH1662-6 (1981), p. 519.

23. C.A. Spindt, I. Brodie, L. Humphrey, and E.R. Westerberg, J. Appl. Phys. 47, 5248 (1976).

24. B. Fell, R.J. Commisso, V.E. Scherrer, and I.M. Vitkovitsky, J. Appl. Physics 53(4), 2818 (1982).

25. L.A. Miles, E.E. Nolting, I.M. Vitkovitsky, and D. Conte, IEEE Conference Record, 1980 Fourteenth Pulse Power Modulator Symposium, Orlando, FL (1980), p. 68.

26. N.W. Harris, F. O'Neill, and W.T. Whitney, Rev. Sci. Inst. 48, 1042 (1977).

27. R.D. Ford and I.M. Vitkovitsky, NRL Memo Report 3561 (1977).

28. D. Conte, R.D. Ford, W.H. Lupton, and I.M. Vitkovitsky, Proc. 7th Symposium on Engineering Problems in Fusion Research, Knoxville, TN, IEEE Pub. 77CH1267-4-NPS (1977), p. 1066.

29. S.A. Genkin, Yu. D. Kosolev, V.G. Rabothin, and A.P. Khuzeiv, Sov. J. Plasma Physics 7(3), 327 (1981).

30. S.C. Brown, *Basic Data of Plasma Physics* (MIT Press, Cambridge, 1967), pp. 87-94.

31. H. Goldstein, *Classical Mechanics* (Addison-Wesley, Reading, 1950), p. 41.

32. R.A. Meger, R.J. Commisso, G. Cooperstein, A.T. Drobot, and Shyke A. Goldstein, 1982 IEEE International Conference on Plasma Science, Ottawa, Canada, IEEE Cat. No. 82CH1770-7 (1982), p. 4.

List of Symbols

A = switch area

E = electric field across the switch

E_B^o = electric field required for breakdown

E_C = electric field across switch during conduction

e = electronic charge

f_o = $eS_o\mu P$

g_b = ratio of beam energy to load energy

g_C = ratio of energy dissipated during switch conduction to load energy

g_O = ratio of energy dissipated during switch opening to load energy

H_b = energy deposited by e-beam in switch gas by inelastic processes

H_C = energy deposited in switch during conduction

H_O = energy deposited in switch during opening

I_b = e-beam current

I_L = load current ($= I_{SW}$)

I_{SW} = switch plasma current

J_b = e-beam current density

J_{SW} = switch plasma current density

k_b = fraction of total e-beam energy deposited in switch gas from inelastic processes

k_O = fraction of load energy dissipated by switch during opening

k_p = ratio of opening time to characteristic loss time for switch plasma

L_o = inductance of storage inductor

L_{SW} = inductance of switch

n = number of pulses

n_p = switch plasma density

P = switch pressure

P_o = atmospheric pressure

r = switch radius

s_B = safety factor for static breakdown

s_H = safety factor for heating

S_o = ionization parameter

v = plasma drift velocity

V_b = e-beam voltage

V_L = voltage across the load

V_{SW} = voltage across the switch

W = energy per unit volume deposited in switch

W_B — energy per unit volume deposited in switch required for breakdown at pressure P

W_B^o — energy per unit volume deposited in switch required for breakdown at atmospheric pressure

ϵ — current gain

ϵ_v — energy required for combination per electron-ion pair

η — switch efficiency

μ — electron mobility

ξ — gain factor

ρ_o — switch resistivity at peak current

τ_C — time interval during which switch is conducting

τ_{CH} — capacitor charging time

τ_{CH}^o — inductor charging time

τ_{COM} — commutation time

τ_L — load pulse width ($\simeq \tau_C$ for closing switch; $\simeq \tau_{NC}$ for opening switch)

τ_{NC} — time interval during which switch is not conducting

τ_p — characteristic loss time for plasma electrons

τ_O — time interval during which switch changes from conducting to nonconducting

τ_{pp} — time interval between pulses

τ_R — rise time of load pulse

τ_{SR} — time interval during which switch change from nonconducting to conducting

END